Remote Sensing of Shaded Area in Vineyards

Lee Johnson[1] and Thibaut Scholasch[2]

ADDITIONAL INDEX WORDS. grape, NDVI, transpiration, irrigation, crop coefficient, *Vitis vinifera*

SUMMARY. **Airborne multispectral image data were compared with intercepted photosynthetic photon flux (*PPF*) in commercial winegrape (*Vitis vinifera*) vineyards of Napa Valley, Calif. An empirically based calibration was applied to transform raw image pixel values to surface reflectance. Reflectance data from the red and near-infrared spectral regions were combined into a normalized difference vegetation index. Strong linear response was observed between the vegetation index and *PPF* interception ranging from 0.15 to 0.50. Study results suggest the possibility of using optical remote sensing to monitor and map vineyard shaded area, thus providing spatially explicit input to water budget models that invoke evapotranspiration crop coefficient based calculations.**

Premium wine production is a fusion of viticulture and enology. The viticultural aspect is becoming increasingly information-intensive as growers seek to maximize the potential of their lands, and enologists seek to optimize fruit sampling strategies with regard to vineyard variability. California winegrapes are a high-value irrigated crop, and investments that boost fruit quality can provide substantial economic returns. As multispectral remote sensing data become increasingly available worldwide for resource monitoring, commercial viticulturists are expanding their use of digital imagery for canopy management decision support (Aho, 2002; Hall et al., 2002; Johnson et al., 2001).

Vineyard irrigation and resulting water status affect several key cropping aspects, including ripening rate (Winkler, 1958), yield and fruit composition (Smart, 1985; Williams and Matthews, 1990), and susceptibility to infestation or disease (English et al., 1989). Water deficits have neutral to negative impact on yield but, if strategically imposed by deficit irrigation, can be used for grape quality enhancement, canopy regulation, and water conservation (Goodwin, 1995; Prichard et al., 2003; Williams, 2001). Accurate water budget characterization is especially crucial under deficit irrigation, as excessive stress can diminish or destroy fruit quality.

Crop coefficient (Kc) based methodologies referred to as FAO-24 (Doorenbos and Pruitt, 1977) and its update FAO-56 (Allen et al., 1998) underpin models that growers can use to track water budget for operational irrigation management in well-watered and deficit-irrigated crops (Goldhamer and Snyder, 1989; Hatfield and Fuchs, 1990). The Kc is the ratio of crop evapotranspiration (ET) to reference ET derived by monitoring of a standardized surface. The California Irrigation Management Information System (CIMIS), for instance, provides daily reference ET updates to growers statewide based on a well-watered, actively growing grass that completely shades the soil surface. Field research has shown that size of the crop canopy at hand, expressed as the proportion of soil shaded near solar noon, is related to Kc in grape (Peacock et al., 1987; Prichard et al., 2003; Williams, 2001) and several other row crops (Grattan et al., 1998).

Vegetation indices derived from spectral data in the red and near infrared (NIR) regions form a basis for evaluation and mapping of vegetation canopy size, both in terms of leaf area index (LAI) and percent cover (Carlson and Ripley, 1997; Wiegand et al., 1991). The indices draw on the fact that, relative to typical soil backgrounds, vegetation canopies are strong scatterers of near-infrared (NIR) energy and strong absorbers of visible energy (Asrar et al., 1984). One common formulation is the normalized difference vegetation index (NDVI), derived from spectral band reflectance (R) as the quantity $(R_{NIR} - R_{red})/(R_{NIR} + R_{red})$. The index generally ranges from 0–1 for vegetated surfaces, with higher values corresponding to greater biomass. The response of NDVI is linear for relatively low LAI canopies, such as those of coastal California vineyards (<2.5 m^2 of leaf per square meter of ground). This relationship was previously merged with vine density information to map leaf area on a per-vine basis in vineyards, using high-resolution satellite imagery (Johnson et al., 2003).

This paper raises the possibility of using digital remote sensing for spatially explicit Kc parameterization of irrigation decision support tools such as CROPWAT (Smith, 1992) and CropSyst (Stockle et al., 2003), based on a linear relationship between airborne NDVI and canopy *PPF* interception observed in mild-climate vineyards. The study builds on the results of Heilman et al. (1982) and Bausch and Neale (1987), who linked Kc with spectral vegetation indices collected by in-situ radiometers in alfalfa (*Medicago sativa*) and corn (*Zea mays*), and also those of Hunsaker et al. (2003) from airborne remote sensing of cotton (*Gossypium hirsutum*).

Methods

STUDY FIELDS. Five small drip-irrigated commercial fields were examined in California's Napa Valley (Table 1). All were located on a 1.5-ha vineyard parcel near Oakville, Calif. (lat. 38°26´N, long. 122°24´W), planted in 1989 with northeast–southwest row orientation. All vines were of cultivar Cabernet Sauvignon, with shoots

[1]Earth Science Div., NASA/ARC 242-4, Moffett Field, CA 94035-1000. To whom reprint requests should be addressed: phone: 650-604-3331; fax: 650-604-4680; e-mail address: ljohnson@mail.arc.nasa.gov

[2]Robert Mondavi Winery, Highway 29, Oakville, CA 94562. Current address: Department of Civil and Environmental Engineering, University of California, Berkeley.

Units

To convert U.S. to SI, multiply by	U.S. unit	SI unit	To convert SI to U.S., multiply by
0.4047	acre(s)	ha	2.4711
0.3048	ft	m	3.2808
0.0929	ft²	m²	10.7639
2.5400	inch(es)	cm	0.3937
1.6093	mile(s)	km	0.6214

Table 1. Physical characteristics of Napa Valley winegrape vineyards used in this study. The fields are ordered by ascending shaded area proportion as per Table 2. All fields were planted to 'Cabernet Sauvignon' in 1989, with vines grouped along northeast–southwest rows.

Field	Rootstock[z]	Trellis[y]	Within-row spacing (m)[x]	Between-row spacing (m)	Plot size (ha)[w]
a	5C	VSP	1.5	2.7	0.20
b	110R	VSP	1.5	2.7	0.28
c	110R	VSP	1.5	2.7	0.16
d	110R	VSP	1.0	1.0	0.13
e	110R	S	1.5	2.7	0.12

[z]Rootstocks = 'Teleki 5C' (*Vitis berlandieri* x *V. riparia*) or '110 Richter' (*V. berlandieri* x *V. rupestris*).
[y]Trellis = VSP (vertically shoot positioned) or S (split canopy).
[x]1 m = 3.2808 ft.
[w]1 ha = 2.4711 acres.

pruned annually to the second node during dormancy. Clean cultivation was practiced throughout, resulting in exposure of bare soil between vine rows. The fields were selected to represent a broad range of canopy size, approaching the full range of development that is encountered in mature, fruit-producing California coastal vineyards under typical management practice (D. Bosch, personal communication).

SHADED AREA ESTIMATION. Measurements of *PPF* interception, or shaded area (SA), were made by a simple and quick canopy evaluation method as currently recommended to growers by agricultural extension agents (Fig. 1). One investigator used a steel tape to measure the width of the shade zone, perpendicular to the row direction, at 10 random locations along one 50-m transect per field (Grattan et al., 1998). A second investigator used a consumer-grade, 3-megapixel digital camera to capture nadir-view photographs of a 18 × 18-inch white board placed within the shade zone at three random locations per transect.

Shaded area is a temporally dynamic phenomenon that is sensitive to changes in solar angle. To support the internal consistency of the dataset, all observations were made within a 20-min period centered on solar noon. Solar elevation during this time period was nearly constant, ranging from 72.3 to 72.6°. The data were taken under clear sky conditions on 18 July 2003. By this date, the vines had reached climax LAI, where they were maintained through September harvest (D. Bosch, personal communication).

The photographs were post-processed with Photoshop software (Adobe Systems, San Jose, Calif.) to estimate and correct for sunflecks (patches of unintercepted sunlight) contained within the shade zone. A threshold brightness level was applied to force darker areas (shade) to black, and brighter areas (sunflecks) to white. A histogram was then used to derive sunfleck proportion per photograph. Shaded area proportions were estimated per field as SA = $z/r \times (1 - s)$, where z was mean shade zone width, r was between-row spacing, and s was mean sunfleck proportion.

IMAGE ACQUISITION. A multispectral image of the study area was acquired under clear sky near solar noon on 8 Aug. 2003 (solar elevation 67.4°) with an airborne camera system (ADAR 5500; Positive Systems, Whitefish, Mont.). The system included four approximately boresighted monochrome cameras (model DCS-420; Kodak, Rochester, N.Y.), respectively fitted with filters in the blue (400–500 nm), green (500–600 nm), red (600–700 nm), and NIR (700–900 nm) spectral regions (Blonski et al., 2000). Flight altitude was 4000 m above ground level, yielding 2 × 3 km total field of view per scene, with 2 × 2-m pixel resolution. The system performed 8-bit analog-to-digital quantization, thereby assigning pixel values of maximum range 0–255 per spectral channel. Translation between scene brightness and pixel value was governed by shutter speed, which was independently set in-flight for each channel based upon brightness histograms from the corresponding camera. The channels were precisely co-registered by

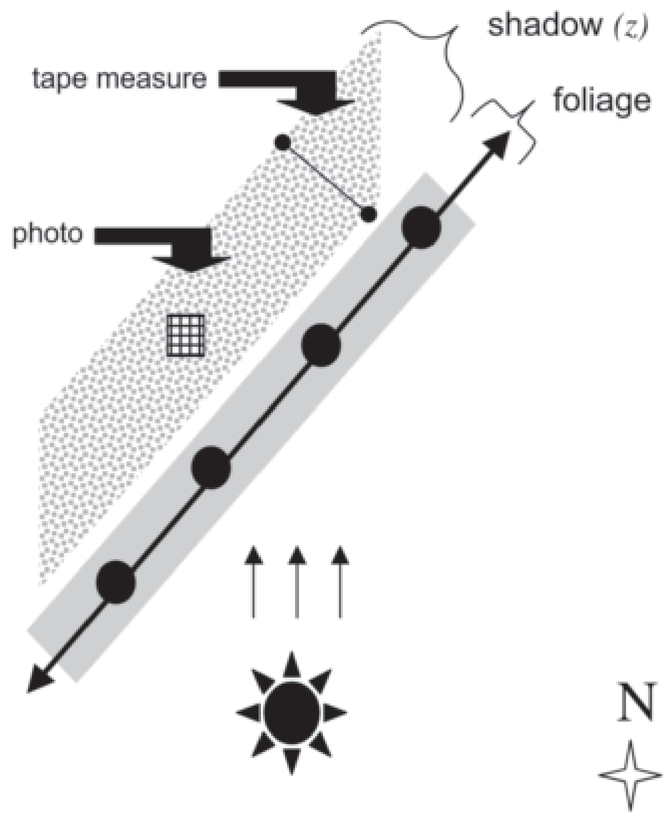

Fig. 1. This top-view schematic shows the strategy for measurement of shaded area proportion within each winegrape vineyard included in this study. Ten measurements of shade zone width (z) were made with a steel tape. Three digital photographs, taken of an 18 × 18-inch (45.7 cm) white board placed at random locations along each transect, were used to correct for the presence of sunflecks with the shade zone. All measurements were made within 10 min of solar noon.

routine pre-processing conducted by the image provider, and the scene was then registered to the California State Plane coordinate system by matching with a 1-m resolution Digital Ortho Quarter Quad (U.S. Geological Survey, Reston, Va.). Although the image was not acquired until 21 d after the SA fieldwork was performed, the LAI was assumed to be unchanged. However, the 5° difference in solar elevation between fieldwork and flight dates likely resulted in a slight downward bias of the measured SA values with respect to actual conditions at the time of image collection.

Image data calibration. A handheld field spectroradiometer (GER 1500; Spectra Vista Corp., Poughkeepsie, N.Y.) was used to develop an empirical basis for conversion of pixel values to surface reflectance (Stow et al., 1996). The GER collects data throughout the visible and NIR with 512 spectral channels at 1.5-nm bandwidth. Four artificial surface features within the scene, ranging from relatively dark to relatively bright, were selected as calibration targets: an unlined asphalt road, a gravel parking lot, and two concrete surfaces. A reservoir was used as a dark target, with assumed brightness of 2% in red and zero in the NIR (Lillesand and Kiefer, 1994). Each target was large relative to the image pixel resolution, reasonably uniform, and spectrally flat. Target reflectance at 650 and 800 nm (red and NIR channel centers) was derived as the mean radiometer response from 10 locations within each target, normalized to ambient light levels by response from a 45 × 45-cm Spectralon reference panel with known reflectance properties. All data were acquired under clear sky near solar noon on 26 Aug. 2003. Although the measurements occurred 18 d post-flight, the target reflectance levels were temporally invariant to first approximation and could therefore be applied to imagery of essentially any date.

Mean red and NIR pixel values corresponding to each target were calculated from nine "pure" pixels (i.e., containing spectral contribution only from the target of interest), extracted as a 3 × 3-pixel array situated in the target center. The asphalt road was too narrow to support such a scheme without introduction of mixed pixels (contaminated by spectral contributions from areas external to the target). Thus, for this case, pure pixels were extracted in essentially linear fashion from along the road center.

Image data extraction. Mean red and NIR pixel values were calculated and recorded for each study field using the area-of-interest tool in the Imagine software package (ERDAS, Atlanta). In specifying the area of interest for these calculations, care was taken to avoid pixels located near any of the study field boundaries. For additional reference, mean pixel values were extracted from bare soil adjacent to the study fields.

Results and discussion

Mean reflectance of the calibration targets ranged from 8.9% to 56.2% in red, and 10.5% to 59.5% in the NIR. Linear relationships were found between target reflectance (R) and image pixel value in the red and NIR channels (Fig. 2). The resulting calibration equations were used to convert mean pixel value (P) from each study field to surface reflectance, as $R_{red} = 0.16 \times P_{red} - 2.67$, and $R_{NIR} = 0.35 \times P_{NIR} - 9.26$. These reflectance values were subsequently combined into per-field NDVI.

Mean SA within the study fields ranged from 0.14 to 0.50 (Table 2). The NDVI values were linearly related to study field SA, with y-intercept approximating sunlit soil NDVI (Fig. 3). As vineyard canopies in this relatively mild temperature region are physically trained to minimize canopy self-shading, SA tends to be directly proportional to LAI. This circumstance forms a basis for linkage of SA and NDVI through leaf display. The linkage is reinforced by the reflectance characteristics of exposed soil. Due to proportionally greater canopy transmittance of NIR energy relative to red, canopy-shaded soil exhibits elevated

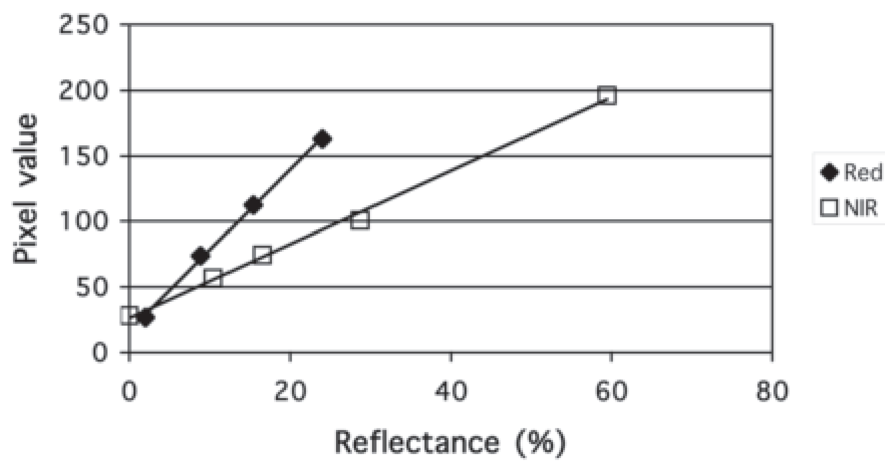

Fig. 2. The reflectance of various surfaces (water, asphalt, gravel, concrete) used for image calibration, measured by a field radiometer, is compared with corresponding pixel values from airborne image red and near-infrared (NIR) spectral channels. The higher slope for the red channel compensates for the relatively low reflectance (typically <15%) of vegetation in that spectral region. The brightest ground target (white concrete) saturated the airborne camera's red channel and was therefore excluded from calibration of that band.

Table 2. Ground-based measurements of shaded area proportion within each vineyard are shown, along with supporting data on width of the shade zone (Fig. 1) and proportion of the shade zone exhibiting sunflecks resulting from sunlight passing through gaps in the canopy.

Field	Shade zone width (m)[z]	Sunfleck proportion	Shaded area
a	0.44	0.10	0.14
b	0.62	0.07	0.25
c	0.69	0.08	0.26
d	0.34	0.09	0.32
e	1.55	0.12	0.50

[z]1 m = 3.2808 ft.

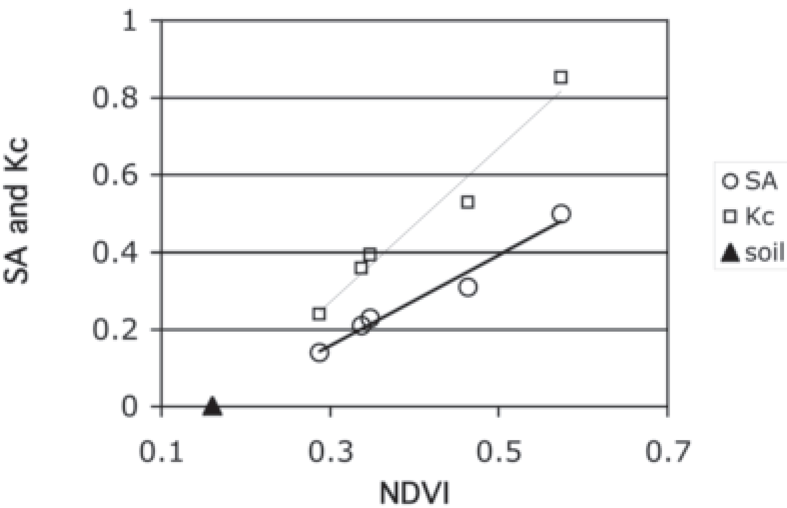

Fig. 3. The relationship between the normalized difference vegetation index (NDVI), derived from red and near-infrared channels of airborne multispectral imagery, and ground-based measurement of shaded area (SA) proportion, is shown for five winegrape vineyards examined in this study. Also shown: SA converted to crop coefficient (Kc) per an empirical relationship (Kc = 1.7 × SA) reported by Williams (2000, 2001). The Kc expresses crop evapotranspiration relative to that of a standardized grass canopy completely shading the soil. A data point for sunlit soil is shown for reference.

NDVI values with respect to sunlit soil. For instance, spectroradiometer measurements taken in this study retrieved NDVI values for sunlit soil near 0.15 (consistent with the airborne measurement of Fig. 3), and near 0.50 for canopy-shaded soil.

Published crop coefficients are generally expressed for a particular crop type as a function of time from planting date or budbreak (e.g., Doorenboos and Pruitt, 1977; Goldhamer and Snyder, 1989). Coefficient seasonal profiles are generally developed from spatially and temporally specific crop ET studies, often involving the use of a weighing lysimeter. Use of these generic profiles, while convenient, may fail to account for the influence of actual growing conditions and management practices related to the specific crop at-hand (Grattan et al., 1998; Neale et al., 2003; Pinter et al., 2003). Misapplication of irrigation may result, serving to reduce farm profitability. Over-irrigation inflates water and energy costs, while potentially reducing winegrape quality. Under-irrigation can diminish both quality and yield.

Derivation of crop coefficients from biophysical observations of canopy size can improve consideration of actual agro-meteorological conditions, thereby supporting customized and possibly more optimized water management strategy. For large properties, or those with highly variable growing conditions, it may be impractical to collect sufficient ground-based point measurements to support operational irrigation scheduling. In the case of SA, internally consistent datasets may be especially challenging to compile due to the variable's dynamic nature. The initial results presented here, if borne out by further testing, suggest that remote sensing technology may offer a viable, highly efficient data collection mechanism for derivation or adjustment of crop coefficients in coastal California vineyards.

Literature cited

Aho, J.E. 2002. NASA providing new perspectives on vineyard management. Vineyard Winery Mgt. 28(2):74–77.

Allen, R.G., D. Raes, and M. Smith. 1998. Crop evapotranspiration—Guidelines for computing crop water requirements. Irr. Drainage Paper No. 56. United Nations Food Agr. Org., Rome.

Asrar, G., M. Fuchs, E.T. Kanemasu, and J.L. Hatfield. 1984. Estimating absorbed photosynthetic radiation and leaf area index from spectral reflectance in wheat. Agron. J. 76:300–306.

Bausch, W. and C. Neale. 1987. Crop coefficients derived from reflected canopy radiation: A concept. Trans. Amer. Soc. Agr. Eng. 30:703–709.

Blonski, S., K. Macey, and C. Schera. 2000. Functional flight test report for Positive Systems' ADAR System 5500 Sensor. NASA John C. Stennis Space Ctr., Miss.

Carlson, T.N. and D.A. Ripley. 1997. On the relation between NDVI, fractional vegetation cover, and leaf area index. Remote Sensing Environ. 62:241–252.

Doorenbos, J. and W. Pruitt. 1977. Guidelines for predicting crop water requirements. Irr. Drainage Paper No. 24. United Nations Food Agr. Org., Rome.

English, J.T., C.S. Thomas, J.J. Marois, and W.D. Gubler. 1989. Microclimates of grapevine canopies associated with leaf removal and control of botrytis bunch rot. Phytopathology 79:395–401.

Goldhamer, D.A. and R.L. Snyder (eds.). 1989. Irrigation scheduling: A guide for efficient on-farm water management. Pub. 21454, Univ. California Div. Agr. and Natural Resources, Oakland.

Goodwin, I. 1995. Irrigation of vineyards: A winegrape grower's guide to irrigation scheduling and regulated deficit irrigation. Inst. Sustainable Irr. Agr., Tatura, Australia.

Grattan, S.R., W. Bowers, A. Dong, R.L. Snyder, J.J. Carroll, and W. George. 1998. New crop coefficients estimate water use of vegetables, row crops. California Agr. 52:16–21.

Hall, A., D.W. Lamb, B. Holzapfel, and J. Louis. 2002. Optical remote sensing applications in viticulture: A review. Austral. J. Grape Wine Res. 8:36–47.

Hatfield, J.L. and M. Fuchs. 1990. Evapotranspiration models, p. 33–59. In: G.L. Hoffman, T.A. Howell, and K.H. Solomon (eds.). Management of farm irrigation systems. Amer. Soc. Agr. Eng., St. Joseph, Mich.

Heilman, J., W. Heilman, and D. Moore. 1982. Evaluating the crop coefficient using spectral reflectance. Agron. J. 74:967–971.

Hunsaker, D.J., P.J. Pinter, E.M. Barnes, and B.A. Kimball. 2003. Estimating cotton evapotranspiration crop coefficients with a multispectral vegetation index. Irr. Sci. 22:95–104.

Johnson, L.F., D.F. Bosch, D.C. Williams, and B.M. Lobitz. 2001. Remote sensing of vineyard management zones: Implications for wine quality. Appl. Eng. Agr. 17:557–560.

Johnson, L.F., D.E. Roczen, S.K. Youkhana, R.R. Nemani, and D.F. Bosch. 2003. Mapping vineyard leaf area with multispectral satellite imagery. Computers Electronics Agr. 38:37–48.

Lillesand, T.M. and R.W. Kiefer. 1994. Remote sensing and image interpretation. 3rd ed. Wiley, New York.

Neale, C.M., H, Jayanthi, and J. Wright. 2003. Crop and irrigation water management using high resolution airborne remote sensing. Proc. Intl. Commission on Irr. and Drainage (ICID) Wkshp. on Remote Sensing of ET for Large Regions, Session 4, United Nations Food Agr. Org., Rome. 7 June 2005. <http://www.kimberly.uidaho.edu/water/montpellier>

Peacock, W.L., L.P. Christensen, and H.L. Andris. 1987. Development of a drip irrigation schedule for average-canopy vineyards in the San Joaquin Valley. Amer. J. Enol. Viticult. 38:113–119.

Pinter, P.J., J.L. Hatfield, J.S. Schepers, E.M. Barnes, M.S. Moran, C.S.T. Daughtry, and D.R. Upchurch. 2003. Remote sensing for crop management. Photogrammetric Eng. Remote Sensing 69:647–664.

Prichard, T., B. Hanson, L. Schwankl, P. Verdegaal, and R. Smith. 2003. Irrigation of quality winegrapes using micro-irrigation techniques. Univ. California Coop. Ext., Davis.

Smart, R.E. 1985. Principles of grapevine canopy microclimate manipulation with implications for yield and quality. Amer. J. Enol. Viticult. 36:230–239.

Smith, M. 1992. CROPWAT: A computer program for irrigation planning and management. Irr. and Drainage Paper No. 46. United Nations, FAO, Rome.

Stockle, C.O., M. Donatelli, and R. Nelson. 2003. CropSyst, a cropping systems simulation model. European J. Agron. 18:289–307.

Stow, D., A. Hope, A.T. Nguyen, S. Phinn, and C.A. Benkelman. 1996. Monitoring detailed land surface changes using an airborne multispectral digital camera system. Inst. Electrical and Electronics Eng. (IEEE), Trans. Geoscience Remote Sensing 34:1191–1203.

Wiegand, C.L., A.J. Richardson, D.E. Escobar, and A.H. Gerbermann. 1991. Vegetation indices in crop assessments. Remote Sensing Environ. 35:105–119

Williams, L.E. 2000. Modelling grapevine water use. Rpt. V-207, Amer. Vineyard Foundation, Napa, Calif.

Williams, L.E. 2001. Irrigation of winegrapes in California. Practical Winery Vineyard, Nov./Dec., p. 42–55.

Williams, L.E. and M.A. Matthews. 1990. Grapevine, p. 1019–1055. In: B.A. Stewart and D.R. Nielsen (eds.). Irrigation of agricultural crops. ASA–CSSA–SSSA, Madison, Wis.

Winkler, A.J. 1958. The relation of leaf area and climate to vine performance and grape quality. Amer. J. Enol. Viticult. 9:10–23.